Dosimetric properties of potassium magnesium borate glass doped with copper

N. Y. Abdou[1], Nabil El-Faramawy[2], and W. M. Abd-Allah[3,*] ⓘ

[1] *Radiation Protection and Civil Defense Department, Nuclear Research Center, Egyptian Atomic Energy Authority (EAEA), Cairo 11371, Egypt*

[2] *Department of Physics, Faculty of Science, Ain Shams University, Abbassia, Cairo 11566, Egypt*

[3] *Radiation Chemistry Department, National Center for Radiation Research and Technology, Egyptian Atomic Energy Authority (EAEA), Cairo 11371, Egypt*

ABSTRACT

The present article deals with potassium magnesium borate glass activated with copper that was prepared by a melting quenching technique to study the feasibility of this glass as a radiation dosimeter. The prepared glasses were characterized through X-ray diffraction and FTIR spectroscopy and some of the glasses optical and physical parameters have been interpreted. The thermoluminescence properties of the prepared samples were studied, and the results revealed that the potassium magnesium borate doped with 0.07 wt% with copper has the highest thermoluminescent response. The glow curve of potassium magnesium borate doped with 0.07 wt% of copper has seven overlapping peaks with maximum temperatures of 383.09, 400.71, 413.26, 426.59, 445.98, 476.57 and 534.04 K, and the TL-response is linear from 0.11 to 165 Gy. From the present study, the potassium magnesium borate doped with 0.07 mol% from copper may be applicable for measuring the radiation dose.

1 Introduction

Nuclear and radiation technology has become one of the most used technologies in many fields, especially in medicine and radiation therapy, where precise dose measurement is needed. Currently, there are several types of radiation detectors available and the thermoluminescent dosimeter is the most important of them [1].

There is a wide range of TL materials in use, and the glassy system is among them. It is particularly appealing for radiation processing applications [2–5]. In recent years, the study of radiation-induced defect centers in glasses has been beneficial in evaluating the quality of glasses for radiation dosimetry applications.

One of the essential glass-forming materials is boron oxide. Because of its high transparency, low cost, low melting point, high sensitivity, great

Address correspondence to E-mail: wesamomar2007@yahoo.com

thermal stability as compared to other TL materials, as it can be present with two groups, tetragonal BO_4 and trigonal BO_3 in the glass sample, the network improves the ability to modify its coordination state from boroxol rings to triangles and tetrahedral BO_4 coordination's appearing short-range structure of triangles BO_3 and tetrahedral BO_4 groups [6–9].

Several attempts to enhance the dosimetric characteristics of borate glass have been performed [10–15]. Several alkali/alkaline metals have been used as modifiers to borate dosimeters over the years [16–18].

Copper is one of the transition metal oxides (TMO) that can exhibit in different oxidation states Cu^{2+}, Cu^+, and Cu^0, which can coexist. The other states of copper ions in the glass matrix led to the intense greenish and bluish color of the glass samples.

Copper is one of the best activators used to enhance the luminescence properties of borate dosimeters as copper can form luminescence centers, which are essential for increasing phosphor strength [18] also, copper has non-hygroscopic nature which increases the chemical stability of borate dosimeters [19].

Upon irradiation, numerous typical defects of borate could appear including boron E-center, non-bridging oxygen NBO's hole centers,which may be clarified as hole center HC, hole trapped on a single NBO, and HC2 hole trapped on two NBO hole center. [20]

The main aim of the present study is to investigate the physical properties of potassium magnesium borate glass doped with copper, such as density, polaron radius, molar volume, average molecular weight, ion concentration, and TL properties, to use it as a high-dose radiation dosimeter.

2 Methodology

2.1 Glass preparation

The glass composition $(70 - x)$ B_2O_3–10 K_2O–20MgO–xCuO, $x = (0.02, 0.07, 0.1, 0.2, 0.5, 1, 1.2$ mol%$)$, was prepared by the melt-quench technique. B_2O_3 was obtained from H_3BO_3, K_2O was obtained from potassium carbonates. MgO and CuO were added as magnesium and copper from each metal oxide (99.99% purity, Alfa). The melt-quench process was used to prepare the mixtures in a porcelain crucible at 1150–1200 °C for 2 h.

2.2 Detailed measuring techniques and calculations for some physical parameter

The Shimadzu X-ray diffractometer was used to assess the condition of the produced glasses within a 2θ angle range of 5° to 60° at 40 kV and 30 mA. Cu Kα radiation and a scan rate of 6° per minute were used to collect data, as well as an X-ray tube. A Bruker's VERTEX 70 FTIR spectrometer was utilized to investigate the spectra of the produced samples at room temperature in the range 4000–400 cm^{-1}, and the absorption spectra of the glasses were recorded. The density (D), molar volume (V_m), oxygen packing density (OPD), the ionic concentrations of the glass samples (N), Internuclear distance (r_i) and polaron of each glass sample were calculated [21, 22].

The density was calculated according to the formula: $\rho = w_a/w_a - w_b \times \rho_o$, where w_a is the weight of the glass sample measured in air, w_b is the weight when the glass is immersed in liquid, and ρ_o is the density of azylene. The molar volume (V_m) was calculated according to the formula $V_m = M/\rho$, where M is the total molecular weight of the multi-component sample. The optical UV–visible absorbance spectra were measured within the UV–visible range (200–1100 nm) using a recording double-beam spectrophotometer (Type JASCO Corp, v-570, Rel-100 Japan) by finely polished glass system.

The Lexsyg Smart TL/OSL luminescent available at the Nuclear Radiation Measurements lab in Department of Physics, Faculty of Science, Ain Shams University was used to measure the glow curve and other TLD—data for the study samples. Lex Studio 2.0 operating software, which runs on a personal computer linked to the reader, controls the reader. The reader is also linked to the nitrogen supply for cooling reasons.

The study samples were irradiated with beta-particles using a beta source of $^{90}S/^{90}Y$, at a dose rate of 110 mGy/s built into the TLD- reader. The result glow curves after being measured were deconvoluted using El-Kinawy TL—software [23].

3 Results and discussion

3.1 Glass characterization

3.1.1 X-ray diffraction (XRD)

As shown in Fig. 1, XRD was carried out on the selected prepared glass sample. It has revealed that peaks of diffraction did not appear. In contrast, only broad bands appeared at around $2\theta = 25°$ for select samples (0, 1.2 mol% CuO), approving the non-crystalline nature of the produced glass.

3.1.2 FTIR spectroscopy

The FTIR analysis of the analyzed samples was optimized to obtain information on the structural units. In this study, it was observed that the vibrational modes of the borate network are mainly active in three infrared spectral regions from 1200 to 1500 cm^{-1} (B–O stretching of trigonal BO_3 units), from 800 to 1200 cm^{-1} (B–O stretching of tetrahedral BO_4 units), and from 600 to 800 cm^{-1} (bending vibrations of various borate segments) [7, 24, 25]. As shown in Fig. 2. The undoped glass reveals several absorption bands extending from the beginning of the measurements at 400 up to 2000 cm^{-1}. The main prominent and characteristic absorption bands usually observed in these three spectral regions are observed at 450, 530, 610, 830, 1070, 1110, 1240, 1380, and 1460 cm^{-1}. The spectral bands in the region of

420–470 cm^{-1} are assigned to specific vibrations of Na–O bonds [26]. The band around 530 cm^{-1} in the region of 500–550 cm^{-1} is assigned to the borate deformation modes [27]. The band located at 700 cm^{-1} is due to B–O–B bending in trigonal BO_3 units [28]. The absorption in the region 650–700 cm^{-1} is attributed to the bending vibrations of B–O–B in BO_3 [26]. The spectral band in the region of 780–1100 cm^{-1} is due to the B–O symmetric stretching of tetrahedral BO_4 units and vibrations of diborates bridging to pentaborate groups [29]. The spectral band in the region of 1200–1300 cm^{-1} is due to the B–O bond stretching vibrations and B–O bridging between B_3O_6 and BO_3 triangles [30]. The band at 1100 cm^{-1} may be due to the stretching vibration of B–O bonds in BO_4 units from tri, tetra, and pentaborate groups [28]. The spectral band in the region 1200–1300 is attributed to anti-symmetrical stretching vibrations with three NBOs of B–O–B groups [31]. Figure 2 also reveals the FT-IR of samples containing progressive addition of CuO. The careful inspection of all the spectral curves before and after doping marked a slight change in the intensity of bands. Some bands of BO_4 groups shifted to a higher wavenumber, while the BO_3 groups were shifted to a lower wavenumber which is in agreement with other research [7, 32, 33]. At the same time, the absorption band becomes broader and accompanied by a shift to a longer wavelength. This may be due to the introduction of CuO transforming some of the BO_3 triangles to BO_4 tetrahedra or vice versa. So, authors used deconvolution method to estimate the fraction of N4 of BO_4 units in the borate network using the Peak Fit program (version 4.12). As shown in Fig. 3a and b and Table 1, for 0 and 1.2 mol% CuO glass sample, they stem from asymmetric stretching vibrational modes of orthoborate, pyroborate, and triangle BO_3 group, respectively. The deconvoluted data of this band also helped to calculate the relative areas of the absorption peaks related to BO_4 and BO_3 groups (N4 and N3, respectively) and the fraction of the four coordinated boron atoms (N4) from the infrared spectra. Besides, the relative area of the deconvoluted bands indicates the variation in N4 in the structure [28, 34]. The tetrahedrally coordinated boron atoms fraction N4, as well as N3, can be calculated using the following formulas:
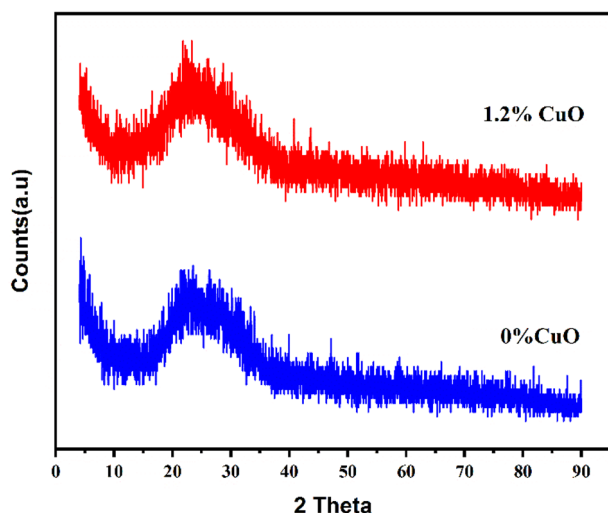

Fig. 1 The XRD patterns of the selected samples $x = 0$ and 1.2 mol%

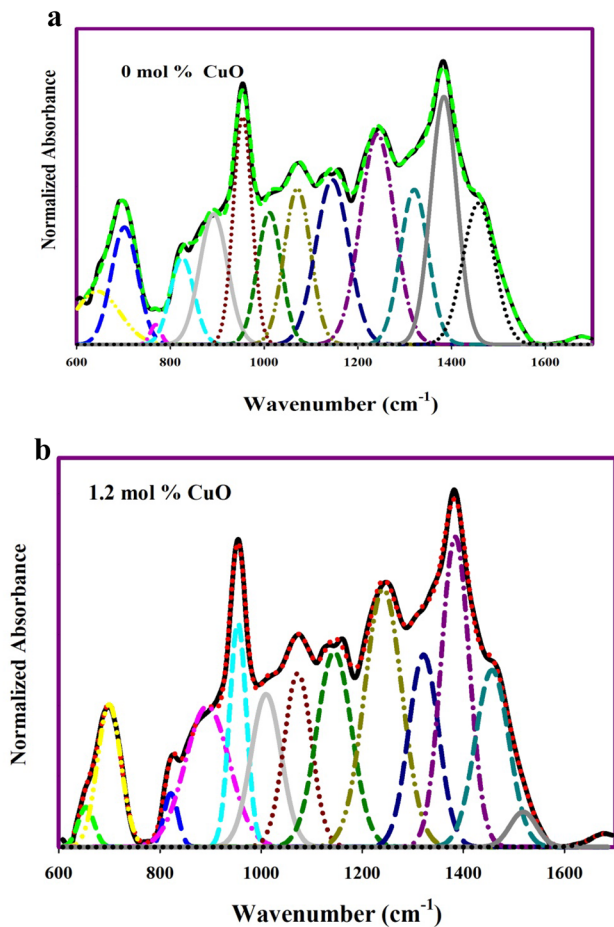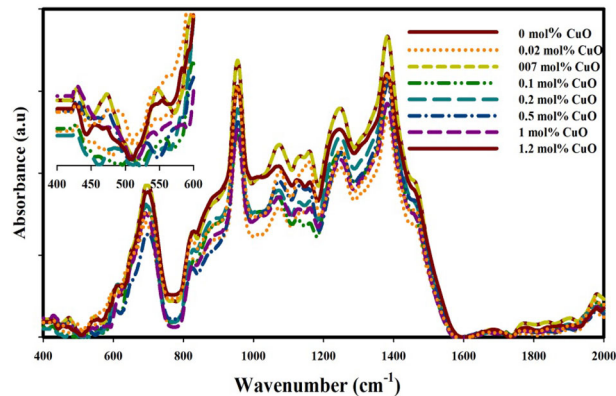**Fig. 2** FTIR absorption
spectra for glass systems

Fig. 3 **a** FTIR deconvoluted absorption spectrum of undoped
glass system. **b** FTIR deconvoluted absorption spectrum of 1.2%
CuO-doped glass system

$$N4 = \frac{\mathrm{concentration\,of\,BO_4}}{\mathrm{concentration\,of\,BO_4} + \mathrm{concentration\,of\,BO_3}} \quad (1)$$

$$N3 = \frac{\mathrm{concentration\,of\,BO_3}}{\mathrm{concentration\,of\,BO_4} + \mathrm{concentration\,of\,BO_3}} \quad (2)$$

where N3 and N4 represent the area of peaks corresponding to BO_3 and BO_4 groups. Figure 4 shows the relation between copper oxide concentration and N4 content, indicating that N4 in a glass is reduced as the copper oxide level rises. On the contrary, N3 increases with increasing the copper oxide content. It can be shown that increasing the copper oxide level significantly influences increasing NBOs. The negative charge on NBOs makes it easier for electrons to be excited at longer wavelengths [7, 35, 36]. The above arguments suggest that the N4 ratio is the most prominent factor in increasing density and decreasing molar volume.

3.2 Density and other parameters

The addition of copper oxide to the glass network may cause some changes in the structure. These changes include rearrangement of the atoms, coordination numbers of the constituents, and variations in the geometrical configuration of the glass that are directly affected by the density. The investigated glass density was changed with the increment in the content of CuO at the expense of the B_2O_3 content, as shown in Fig. 5. The increase in density might be due to the substitution of lower atomic mass ($B_2O_3 = 69.62$) with higher atomic mass (CuO = 79.547). It is possible that most of the Cu ions enter the glass samples network as a modifier, which

Table 1 The curve fitting parameters (the band centers C and the relative area (A) for the glass systems

mol% CuO		Band centers C and relative areas A
0 mol%	C	646 702 759 827 887 954 1019 1075 1149 1243 1319 1384 1460 1525 1678
	A	3.79 5.80 1.03 4.05 5.79 10.50 5.71 7.86 10.59 13.41 8.38 13.16 8.49 1.08 0.38
0.02 mol%	C	690 847 959 1100 1234 1377 1484 1656
	A	7.27 4.34 19.84 15.56 19.50 27.95 5.27 0.27
0.07 mol%	C	691 825 891 953 1053 1157 1244 1323 1382 1451 1678
	A	9.58 3.44 6.26 5.70 19.61 6.48 12.16 8.14 8.71 11.66 0.34
0.1 mol%	C	605 658 702 740 831 895 954 1013 1070 1119 1162 1219 1262 1321 1381 1454 1682
	A	0.33 2.41 4.98 0.42 2.97 6.23 8.27 6.55 7.00 5.15 6.07 7.18 7.60 9.24 11.83 13.03 0.73
0.2 mol%	C	655 698 824 867 909 954 1006 1047 1082 1125 1165 1214 1254 1301 1343 1383 1423
	A	0.65 5.09 1.65 3.47 3.71 8.92 5.25 4.00 5.63 5.41 5.58 6.46 7.10 7.53 6.56 6.10 10.08
0.5 mol%	C	653 700 759 823 868 910 955 1006 1046 1082 1125 1165 1214 1254 1301 1343 1383 1423 1467 1546
	A	1.29 5.37 0.31 2.27 3.57 3.75 8.42 5.19 4.00 5.44 5.27 5.46 6.23 7.15 7.15 6.76 9.36 5.85 5.05 0.34
1 mol%	C	653 700 759 823 868 910 955 1006 1046 1082 1125 1165 1214 1254 1301 1343 1383 1423 1467 1508 1648 1685
	A	1.29 5.37 0.31 2.27 3.57 3.75 8.42 5.19 4.00 5.44 5.27 5.46 6.23 7.15 7.15 6.76 9.36 5.85 4.95 2.23 0.17 0.40
1.2 mol%	C	655 700 736 825 887 954 1017 1074 1126 1165 1215 1257 1317 1384 1456 1511 1547 1681
	A	1.41 5.14 0.32 2.43 6.58 9.70 6.14 8.09 5.15 5.29 6.27 7.67 10.02 14.64 8.57 1.71 0.23 0.63

consolidates their structure and raises their density [7, 28].

In the current work, the molar volume and the density display opposite behavior, which is the normal trend [28, 37].

The following relationship can expect the ion concentration of Cu as given in Table 2:

$$Cu = \left(\frac{6.023 \times 10^{23} \times \text{mol fraction of cation} \times \text{Valency of cation}}{V_m} \right) \tag{3}$$

According to the current study, Cu ion concentration values increase with increasing the Cu content. This increase is associated with reductions in the molar volume.

The relationship (4) will be used to calculate the interionic distance (r_i) between two Cu ions

$$r_i = \left(\frac{1}{\text{Concentration of Cu}} \right)^{\frac{1}{3}} \tag{4}$$

It was observed that as the concentration of CuO increased, the values of r_i reduced, and this reduction was associated with a decrease in the molar volume.

3.2.1 Optical absorption spectroscopy

Figure 6 shows the UV–Visible optical absorption spectra of the investigated polished glassy samples at room temperature against the 300–1100 nm wavelength. The obtained results of undoped copper are neutral, while the samples doped with copper oxide have a bluish-green color with cumulative copper oxide, then the color changes to dark green. The green color is an indication that the copper has a Cu^{2+} divalent oxidation state. The glass samples have a broad visible band around 780 nm [38], which may be recognized as a d–d transition due to $Cu^{2+}(d^9)$ ions in the octahedral field, owing to the $^2B_{1g} \rightarrow {}^2B_{2g}$ octahedral transition of Cu^{2+} ions [28]. The peak position is shifted toward higher wavelengths due to the ligand field around the Cu^{2+} ion. An electronic hole in the degenerated orbital disturbs the Cu^{2+} ions, causing the tetragonal distortion. The E_g optical bandgap values with the concentration of Cu^{2+} are listed in Table 2.
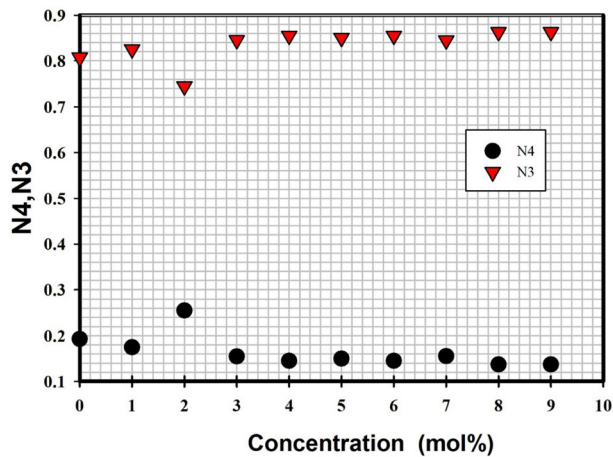
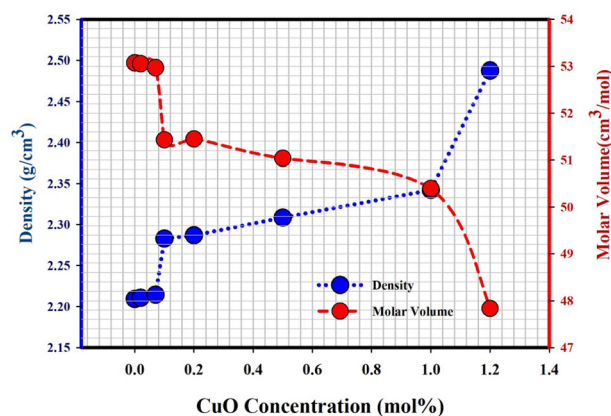**Fig. 4** The relation between N3 and N4 of glass samples

Fig. 5 Density (ρ) dependence on glass composition and molar volume (V_m) for glass system

3.2.2 Some physical parameters

Optical bandgap energy (E_{opt}), for indirect transitions, is sensitive to bonding between atoms. Energy gap calculations match those of Davis and Mott [39]. $(\alpha h v)^{1/2} = B(h v - E_g)$, where $h v$ is the incident photon energy, B is the band tailing parameter constant, and E_g is the optical bandgap energy. The optical band gap value can be detected in Fig. 7, and the values are listed in Table 2. It was noticed that the optical bandgap energy values were reduced by increasing the concentration of Cu^{2+} at the expense of B_2O_3. This reduction allowed a decrease in the width of the localized states (γ) values and the average binding energy (cohesive energy). These are the main factors in increasing the number of free electrons less tightly linked to the nuclear charge. Free electrons can move from the valence band to the conduction band,

decreasing the E_g optical bandgap energy. The refractive index (n) was valued from the values of E_{opt} using the following relation proposed by glass scientists [40, 41]: $\frac{n^2-1}{n^2+2} = 1 - \sqrt{\frac{E_g}{20}}$. The refractive index values increased with cumulative Cu^{2+} concentration; this caused a rise in the amount of BO_3 and NBO, while BO_4 decreased. This observation can be attributed to the conversation of BO_4 into BO_3 and NBO. The optical electronegativity (χ) has been valued by, $\chi = 0.2688E_g$, where E_g is the bandgap. Thus, the electronegativity (χ) values were reduced with cumulative Cu^{2+} concentration. The optical basicity was $\wedge = -0.5\chi + 1.7$, so the electronegativity (χ) values were reduced through cumulative Cu^{2+} concentration. The electron polarizability has been valued by $\propto° = -0.9\chi + 3.5$. The change in the value of the electronic polarizability by cumulative Cu^{2+-} concentration in the glasses may tend to break down borate bonds to create non-bridging oxygen atoms [42].

The molar refraction R_m is styled by the following Lorentz–Lorenz equation [43]:

$$R_m = V_m \left(1 - \sqrt{\frac{E_g}{20}}\right) \tag{5}$$

R_m is the molar refraction, E_g is the energy bandgap, and V_m is the molar volume.

The findings showed that adding CuO reduced the optical basicity, optical bandgap, and electronegativity while increasing the refractive index. The metallization criterion has been estimated as $M = 1 - R_m/V_m$. Table 2 revealed that the metallization value decreased by adding Cu^{2+}[21, 36].

3.2.3 Thermoluminescent properties

The TL-intensity and glow curve of potassium magnesium borate doped with 0, 0.02, 0.07, 0.1, 0.2, 0.5, 0.7, 1, and 1.2 mol% concentrations of copper after being exposed to β-dose 55 Gy have been investigated, and the results are displayed in Fig. 8a and b.

This result showed that the doping of potassium magnesium borate with copper significantly increased the TL-intensity compared to undoped potassium magnesium borate. The resulted increase in the TL-intensity is dependent on the mol % of copper.

On the other side, the potassium magnesium borate doped with different mol% of copper has the

Table 2 Density, Oxygen packing density (OPD), Molar volume V_m, Ionic concentrations N, Inter-ionic distance r_i, polaron, radius r_p, Distance $d_{B–B}$, Optical energy band gap (E_{opt}) indirect, Refractive index (n), Optical electronegativity χ, Optical basicity ($\wedge$), electron polarazability X, molar refractivity, Metalization (M) for glass system

Properties	CuO concentration							
	0 mol%	0.02 mol%	0.07 mol%	0.1 mol%	0.2 mol%	0.5 mol%	1 mol%	1.2 mol%
Density (ρ) (g/cm^3)	2.20	2.21	2.21	2.28	2.28	2.30	2.34	2.48
OPD (g atom/l)	2.4	2.39	2.39	2.39	2.38	2.38	2.38	2.91
V_m (cm^3/mol)	53.07	53.05	52.97	51.43	51.44	51.03	50.39	47.84
N (MO) (ions/cm^3) $\times 10^{20}$	–	4.54	10.59	20.34	40.73	100.17	200.33	300.02
Ionic radius (r_i) $\times 10^{-22}$	–	7.34	2.09	1.42	0.705	0.28	0.139	0.11
Polaron radius (r_p) $\times 10^{-22}$	–	2.95	0.84	0.59	0.028	0.11	0.57	0.44
Optical bandgap Eg (eV)	3.6	3.16	3.16	3.15	3.12	3.1	2.99	2.92
Refractive index	2.25	2.35	2.35	2.35	2.36	2.37	2.39	2.62
Optical electronegativity χ	0.97	0.85	0.84	0.84	0.84	0.83	0.80	0.78
Optical basicity	1.14	0.943	0.94	0.939	0.925	0.916	0.866	0.83
Electron polarazability 10^{-23} ions/cm^3 ($\propto°$)	1.21	1.26	1.26	1.22	1.23	1.23	1.23	1.23
Molar refractivity R_m (cm^3)	30.5	32	32	31	31	30	30	31
Metallization (M)	0.42	0.39	0.39	0.39	0.39	0.39	0.38	0.33

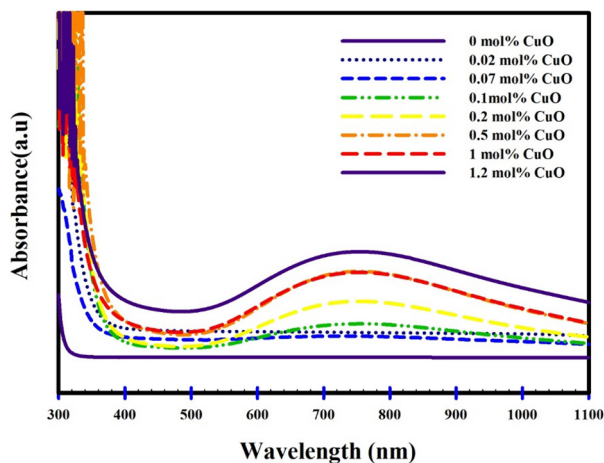**Fig. 6** Absorption spectrum of selected glass samples

Fig. 7 The indirect optical energy gap of selected glass samples

same glow curve structure with one broad peak in the same position at $\approx$ 383.7 K, but the area under the glow curve has changed with the change in the mol% of copper.

The presence of one broad peak in the glow curve of potassium magnesium borate doped with copper means that this peak may be composed of more than one glow peak overlapping with each other. Each peak is specific to one trap in the crystal lattice. The positions of these traps in the crystal lattice of prepared glass are very close to each other. So, when the
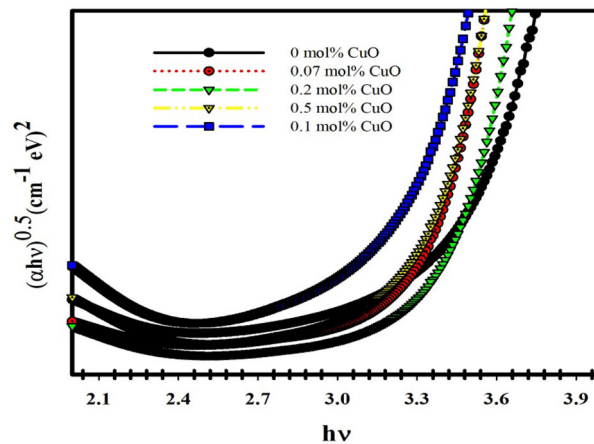
prepared glass was heated during reading, these peaks overlapped and appeared as one peak.

The highest TL-intensity was found in potassium magnesium borate doped with 0.07 mol% of copper. As a result, this specific concentration will be mainly discussed in the following section.

3.2.4 Kinetic parameters

Calculating the kinetic parameters of the electron traps inside the material is necessary to understand its behavior in recording the electrical charges and its

ability to maintain this charge. However, to do this, the number of peaks that make up the curve should first be determined; if the glow curve has overlapping peaks, they must be separated first.

3.2.4.1 T_m–T_{stop} method The T_m–T_{stop} technique [44] was used to determine the predicted number of the glow peaks in the glow curve of potassium magnesium borate doped with 0.07 mol% of copper. For this purpose, we performed the following:

- The samples were irradiated at a dose of 132 Gy of beta particles.
- The glow curve was recorded immediately after irradiation from room temperature to a temperature called T_{stop} (stopping temperature) at a linear heating rate of 5 K/s.
- The samples were cooled to room temperature and reheated to record the whole glow curve up to 723 K with the same linear heating rate.
- The temperature corresponding to the first maximum intensity in obtained glow curve (T_m) was determined.
- The process of heating to a T_{stop} and cooling to room temperature, and then reheating to record the whole glow curve was repeated for different values of T_{stop} ranging from 328 to 648 K, with an increment of 5 K.
- The corresponding T_{stop} and T_m were determined at each heating cycle, and a graph between various values of T_m against T_{stop} was obtained. The results are shown in Fig. 9.

From Fig. 9, the relation between T_m and T_{stop} appeared like a staircase structure where the relation began straight line; then a plateau occurred (flat region), after that, the relation retrained as a straight line, then the plateau region appeared again. The number and location of the plateau regions represent the number and locations of the glow peaks that make up the glow curve. So, the glow curve of potassium magnesium borate doped with copper 0.07 mol% has seven expected peaks at 383.09, 400.71, 413.26, 426.59, 445.98, 476.57, and 534.04 K.

Based on the expected number of glow peaks, the Glow Curve Deconvolution (GCD) was performed using El-Kinawy TL software [23], which determined the activation energy, frequency factor, and kinetic order for each peak after deconvolution. The quality of GCD fit between theoretical and experimental results has been tested with the Figure of Merit
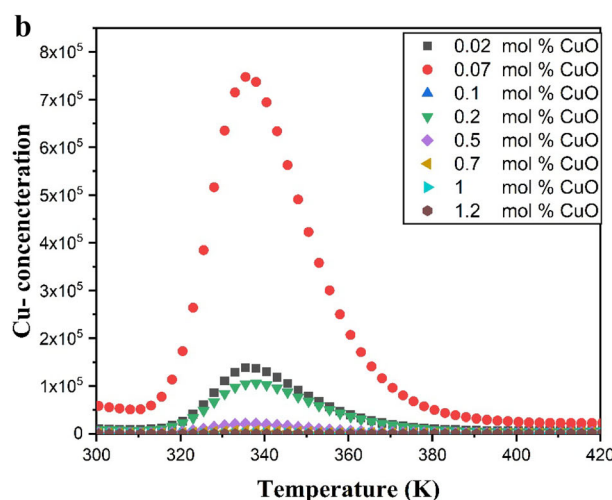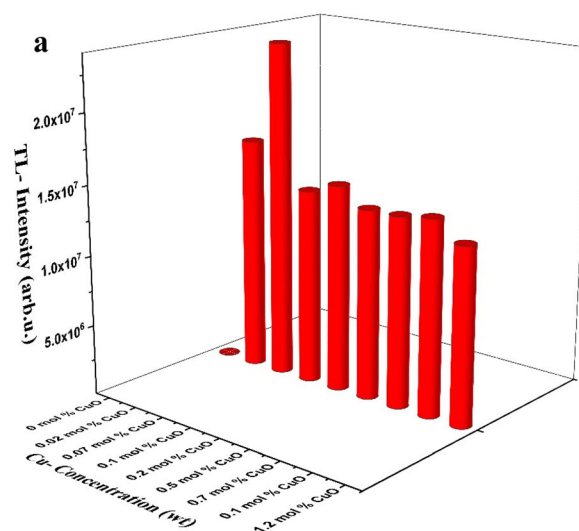
Fig. 8 **a** The effect of different concentrations of Copper on TL—the intensity of Potassium Magnesium Borate. **b** The effect of different concentrations of Copper on the glow curve of Potassium Magnesium Borate

(FOM) [45, 46], as seen in Table 3 and Fig. 10. As shown in Table 3, the FOM value states the goodness of fit, where the values FOM less than 2.5% refer to a good fit [46].

3.2.5 Linearity and dose response

To establish the possibility of any material being used as a measure of radiation dose, it is needed to know the sort of connection between the radiation portion and the reaction of this material to radiation portion. It is favored that this relationship be linear.

The glass system doped with copper 0.07 mol% was exposed to various doses of β-particles from 0.11

to 165 Gy. After that, the TL-response of the irradiated glass system doped with copper 0.07 mol% samples was recorded, and the obtained glow curves corresponding to each dose were deconvoluted by El-Kinawy TL-software [23].

The shape and position of the peaks for the glow curve of the glass system doped with copper 0.07 mol% did not change with the variation in the radiation dose as seen in Fig. 11, except the area under the glow curve and the corresponding TL-intensity increased with increasing the β-particle doses. This may be due to defects caused by β-particles plus the different types of defects already in the glass before irradiation, which causes an increase in the luminescence intensity [47].

Furthermore, increasing β-dose also induces additional luminescence centers. this may be due to the formation of some defects such as, non-bridging boron oxygen hole centers (NBOHC) / boron electron centers (BEC), and boron oxygen hole centers (BOHC).

The total area under the glow curve of the glass system doped with copper 0.07 mol% was plotted as a function of β-doses. The obtained relation was fitted as a linear fit with the expression ($Y = 5.13 + 0.92x$), and the regression square fitting value equalled 0.998. These findings revealed that the glass system doped with copper 0.07 mol% has a linear response from 0.11 up to 165 Gy from β-particle as seen in Fig. 12. The area under each peak after deconvolution of the glow curve was also calculated as a function of beta dose. The results showed that the seven peaks had a linear relationship with the β doses in the range of 0.88 up to 165 Gy and the results are presented in Fig. 13.

3.2.6 Reproducibility

It is necessary to verify the studied sample repeatability to be used as dosimeters to determine their accuracy. The ability to keep the TL response following the repeated use of the same dosimeter at the same applied dosage is referred to as "reproducibility". If the coefficient difference between readings after five to ten cycles is less than 5%, the dosimeter is regarded as having a high repeatability. [48, 49]. Thus, the TL-response of a sample from the glass system doped with copper 0.07 mol% was studied after six cycles of irradiation at 0.22 Gy from β-particles and the results showed that the coefficient difference is 2.21% as shown in Fig. 14. This result showed that the glass system doped with copper 0.07 mol% has a good reproducibility.

3.2.7 Sensitivity

One of the essential features that distinguish a dosimeter is its sensitivity. The sensitivity of the dosimeter could be assessed using Eq. (5) [49].

$$Sensitivity = \frac{TL\text{-}intensity}{(Applied\ dose\ (Gy) \times (Mass\ (mg))} \quad (6)$$

Hence, the sensitivity of the prepared glass system doped with copper 0.07 mol% was calculated using Eq. (6) for dose range from 0.11 up to 165 Gy, and the
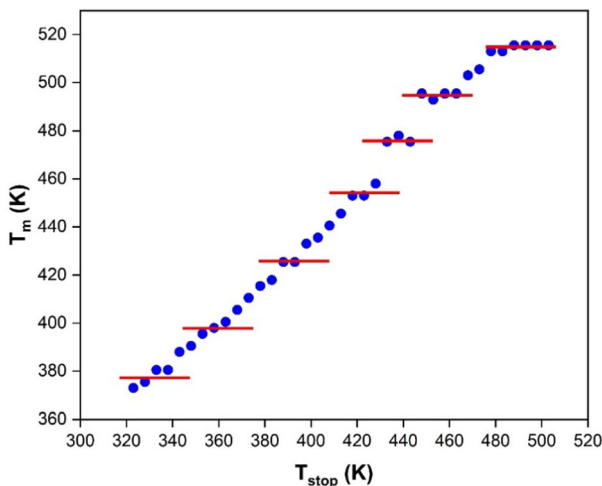

Fig. 9 T_m–T_{stop} results of the glass system doped with copper 0.07 mol%

Table 3 The calculated trapping parameters of the prepared glass system doped with copper 0.07 mol% using CGCD after exposure to 132 Gy

Peak no	T_m (k)	E (ev)	S (s^{-1})	b	FOM %
Peak 1	383.09	0.8	9.11×10^9	1.6	1.8743
Peak 2	400.71	0.9	6.26×10^{10}	1.7	
Peak 3	413.26	1	5.74×10^{10}	1.55	
Peak 4	426.59	1.01	2.53×10^{11}	1.8	
Peak 5	445.98	1.15	3.08×10^{12}	1.6	
Peak 6	476.57	1.2	1.40×10^{12}	1.5	
Peak 7	534.04	1.3	4.50×10^{11}	1.8	
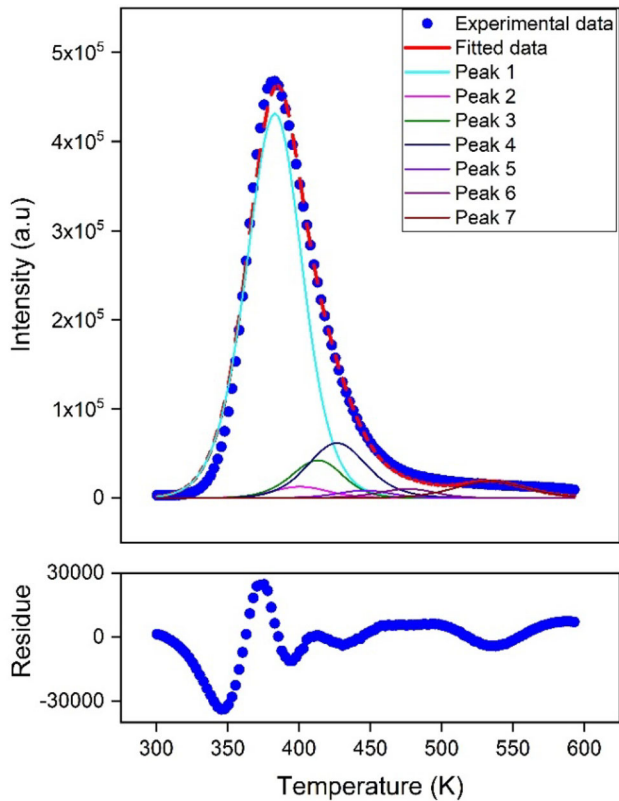
Fig. 10 The glow curve of the glass system doped with copper 0.07 mol% after deconvolution

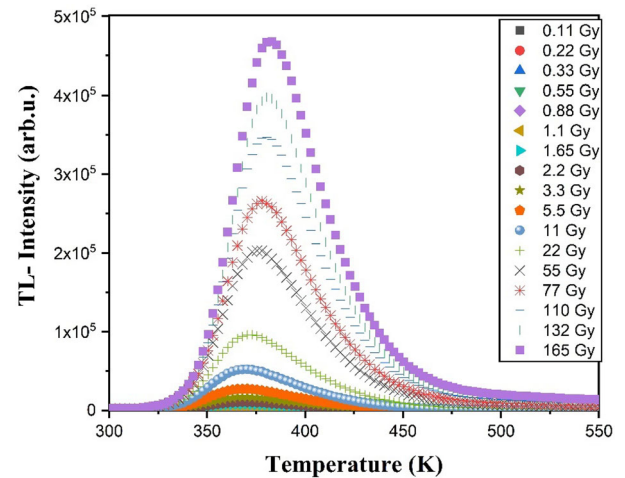**Fig. 11** The effect of different doses of β-particles on the glow curve of the glass system doped with copper 0.07 mol%

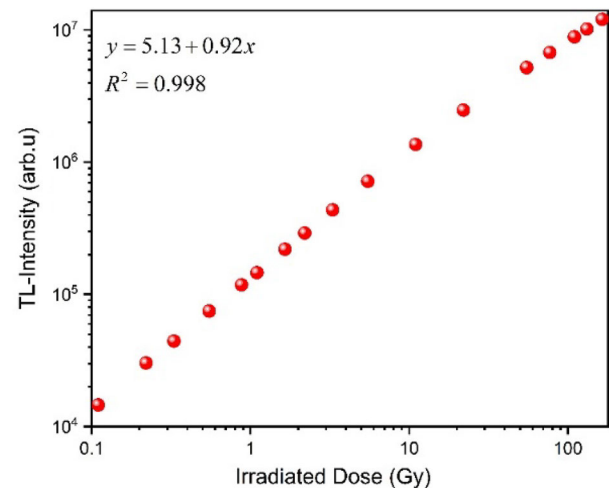**Fig. 12** The dose–response for the glass system doped with copper 0.07 mol%

results are shown in Fig. 15. It could be observed from this result that the sensitivity was decreased as the applied dose increased, where the average sensitivity overall studied dose range was $3309.49 \pm 20\%$.

In addition, the relative sensitivity of the dosimeter could be assessed by comparing the intensity of the studied samples after being exposed to a certain dose with that obtained from a reference dosimeter (LiF, TLD-100) after being exposed to the same dose [49, 50]. Thus, samples from the glass system doped with copper 0.07 mol% and TLD-100 were irradiated at 11 Gy, then the TL-intensity was recorded. The results revealed that TLD-100 has a relative sensitivity of 128.5 times as compared to that of a prepared glass system doped with 0.07 mol% copper (Fig. 15).

3.2.8 Fading

It is critical to understand the degree of electrical charge stabilization within the traps in the dosimeter over time [44]. So, a glass system doped with copper 0.07 mol% sample was irradiated at 11 Gy from β-

particle and stored in the dark at room temperature for an interval time. The results revealed that the residual TL-intensity was 10% after 72 h from the first reading and it remained constant over the remaining studied period of 696 h, as seen in Fig. 16.

The glow peaks at 383.09, 400.71, and 413.26 K disappeared after 72 h from irradiation which explains the quick fading in the first 72 h, hence these peaks are considered lower temperature peaks, however the glow peaks at 426.59, 445.98, 476.57 and 534.04 K remain constant overall the study period.
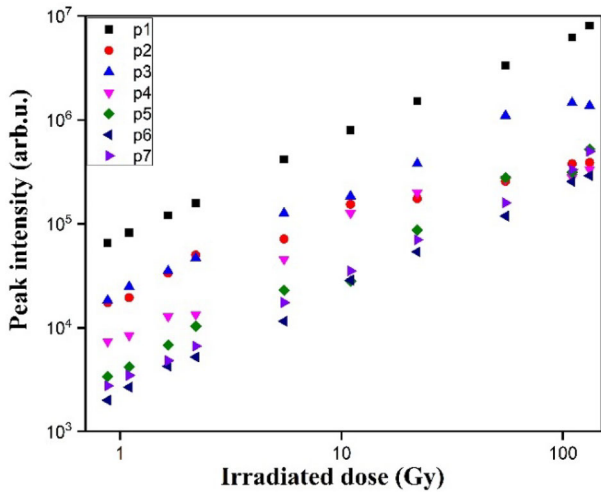
Fig. 13 The dose–response for five peaks of the glass system doped with copper 0.07 mol% after deconvolution
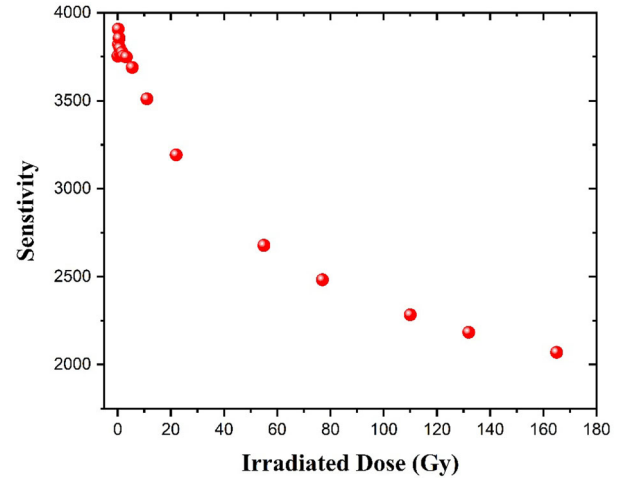

Fig. 15 The sensitivity of the glass system doped with copper 0.07 mol% in the dose range from 0.11 up to 165 Gy
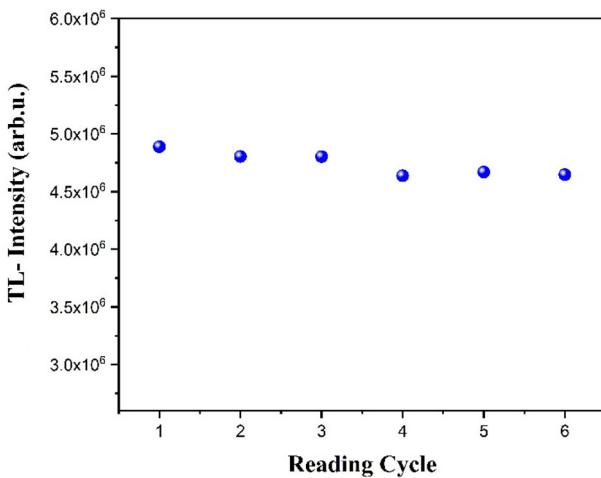

Fig. 14 The reproducibility of the radiation response of the glass system doped with copper 0.07 mol% for six successive cycles
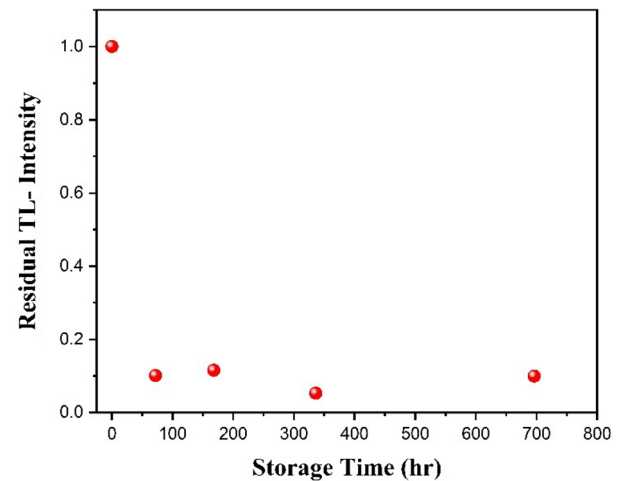

Fig. 16 The residual TL- the intensity of the glass system doped with copper 0.07 mol% after different storage times from irradiation

Thus, it is recommended that when using the prepared glass pre-annealing should be performed before reading to temperature 415 K.

4 Conclusions

Based on the results, it can be concluded that:

- The potassium magnesium borate doped with copper was prepared by a melting quenching technique to study the thermoluminescent behavior after β-particle exposure. According to the results, FTIR and N4 values established the

occurrence of BO_3 and BO_4 groups in the glass network and the addition of CuO until the maximum concentration is reached (1.2 mol%) has no significant effect on the primary distinctive borate groups in the study, but slight changes in the intensities or places of some of the IR bands are identified.

- The density of the glass system showed an increment in the content of CuO increases and molar volume decreases.

- IR spectra reflect characteristic absorption bands due to specific borate network

- The glass system doped with copper 0.07 mol% has the highest TL-response, and its glow curve has seven overlapped peaks at 383.09, 400.71, 413.26, 426.59, 445.98, 476.57 and 534.04 K. The TL-response is linear from 0.11 up to 165 Gy. The coefficient difference for KMB: Cu 0.07 mol% is 3.37% after six irradiation and reading cycles.
- The glass system doped with copper 0.07 mol% fades quickly in the first three days, then they remain stable. The calculated activation energies for seven peaks are 0.80, 0.90, 1, 1.01, 1.15, 1.20 and 1.30.
- The potassium magnesium borate doped with 0.07 mol% copper found in the present work might be used to measure radiation dosage.

Author contributions

All of the authors have taken full responsibility for the content of this manuscript.

Data availability

My manuscript and associated personal data will be shared with Research Square for the delivery of the author dashboard.

Declarations

Conflict of interest The authors declare that they have no conflict of interest. The authors declare that they have no known competing financial interests or personal relationships that could have appeared to influence the work reported in this paper.

Informed consent The authors consent to participate.

Consent for publication The author's consent for publication.

References

1. M. Środa, S. Świontek, W. Gieszczyk, P. Bilski, The effect of CeO2 on the thermal stability, structure and thermoluminescence and optically stimulated luminescence properties of barium borate glass. J. Non-Cryst. Solids **517**, 61–69 (2019)

2. N. Abdou, M. Farag, W. Abd-Allah, Thermoluminescent properties of nano-magnesium phosphate ceramic for radiation dosimetry. Eur Phys J Plus **135**(3), 317 (2020)

3. A. El-Kheshen, C. Woda, M. Discher, N. El-Faramawy, Investigation of phosphate glass doped lanthanum as beta dosimeter. J. Lumin. **200**, 254–259 (2018)

4. H.F. El-Nashar, M. El-Kinawy, N. El-Faramawy, Investigations of the kinetic energy parameters of irradiated (La)-doped phosphate glass. Luminescence **35**(1), 107–113 (2020)

5. H.A. Alazab, N. Abdou, H. Saudi, W. Abd-Allah, Thermoluminescence properties of bioglass for radiation dosimetry. SILICON (2021). https://doi.org/10.1007/s12633-021-01364-1

6. R. Kaur, V. Bhatia, D. Kumar, S. Rao, S.P. Singh, A. Kumar, Physical, structural, optical and thermoluminescence behavior of Dy_2O_3 doped sodium magnesium borosilicate glasses. Results Phys **12**, 827–839 (2019)

7. W. Abd-Allah, E. Nabhan, Effect of CoO and gamma irradiation on the infrared absorption spectra of lithium borate glasses. SILICON **10**(1), 49–57 (2018)

8. S. Hashim, Y. Alajerami, A. Ramli, S. Ghoshal, M. Saleh, A.A. Kadir, M. Saripan, K. Alzimami, D. Bradley, M.

Mhareb, Thermoluminescence dosimetry properties and kinetic parameters of lithium potassium borate glass co-doped with titanium and magnesium oxides. Appl. Radiat. Isot. **91**, 126–130 (2014)

9. B. Mohammed, M. Jaafar, H. Wagiran, Thermoluminescence dosimetry properties and kinetic parameters of zinc borate silica glass doped with Cu_2O and co-doped with SnO_2. J. Lumin. **204**, 375–381 (2018)

10. N. El-Faramawy, S. El-Kameesy, A. Abd El-Hafez, M. Hussein, G. Metwally, Study of thermal treatment and kinetic parameters of prepared Li2B4O7: Cu Thermoluminescence dosimeter. Egypt. J. Sol **23**, 103–111 (2000)

11. W. Ayta, V. Silva, N. Dantas, Thermoluminescent properties of a Li_2O–B_2O_3–Al_2O_3 glass system doped with CaF_2 and Mn. J. Lumin. **130**(6), 1032–1035 (2010)

12. R. Nattudurai, A.K. Raman, C.B. Palan, S.K. Omanwar, Thermoluminescence characteristics of biological tissue equivalent single crystal: europium doped lithium tetraborate for dosimetry applications. J. Mater. Sci.: Mater. Electron. **29**(17), 14427–14434 (2018)

13. N. El-Faramawy, A. El-Naggar, C. Woda, M. El-Kinawy, Dosimetric properties of lithium borate glass doped with dysprosium. Luminescence **36**(1), 210–214 (2021)

14. N. El-Faramawy, A. El-Naggar, C. Woda, M. El-Kinawy, Investigation of TL dosimetric parameters of lithium borate glass doped with dysprosium. Opt. Mater. **113**, 110672 (2021)

15. A. Saidu, H. Wagiran, M. Saeed, Y. Alajerami, A. Kadir, Effect of co-doping of sodium on the thermoluminescence dosimetry properties of copper-doped zinc lithium borate glass system. Appl. Radiat. Isot. **118**, 375–381 (2016)

16. S. Rojas, K. Yukimitu, A. De Camargo, L. Nunes, A. Hernandes, Undoped and calcium doped borate glass system for thermoluminescent dosimeter. J. Non-Cryst. Solids **352**(32–35), 3608–3612 (2006)

17. N.A. Salleh, A.R. Tamuri, M.A. Saeed, Effect of strontium concentration on thermoluminescence glow curve of copper doped lithium magnesium borate glass. Malaysian J. Fund. Appl. Sci. **13**(3), 275–278 (2017)

18. Y. Alajerami, S. Hashim, S. Ghoshal, D. Bradley, M. Mhareb, M. Saleh, Copper doped borate dosimeters revisited. J. Lumin. **155**, 141–148 (2014)

19. H. Aboud, H. Wagiran, R. Hussin, H. Ali, Y. Alajerami, M. Saeed, Thermoluminescence properties of the Cu-doped lithium potassium borate glass. Appl. Radiat. Isot. **90**, 35–39 (2014)

20 I.A. Shkrob, B.M. Tadjikov, A.D. Trifunac, Magnetic resonance studies on radiation-induced point defects in mixed oxide glasses. I. Spin centers in B_2O_3 and alkali borate glasses. J. Non-Cryst. Solids **262**(1–3), 6–34 (2000)

21. H. Saudi, W. Abd-Allah, K.S. Shaaban, Investigation of gamma and neutron shielding parameters for borosilicate glasses doped europium oxide for the immobilization of radioactive waste. J. Mater. Sci.. **31**(9), 6963–6976 (2020)

22. K.S. Shaaban, W. Abd-Allah, Y. Saddeek, Gamma rays interactions with CdO-doped lead silicate glasses. Opt. Quant. Electron. **52**(1), 1–17 (2020)

23. M. El-Kinawy, H.F. El-Nashar, N. El-Faramawy, New designed software to deconvolute the thermoluminescence glow-curves. SN Applied Sciences **1**(8), 1–7 (2019)

24. S. Marzouk, N. Elalaily, F. Ezz-Eldin, W. Abd-Allah, Optical absorption of gamma-irradiated lithium-borate glasses doped with different transition metal oxides. Physica B **382**(1–2), 340–351 (2006)

25. A. Mansour, W. Abd-Allah, N. El-Alaily, F. Ezz-Eldin, Study of paramagnetic species in γ-irradiated lithium borate glasses doped with Cu^{2+} ions. J. Nucl. Technol. Appl. Sci. **1**(4), 497–509 (2013)

26. R.L. Frost, R. Scholz, A. López, Y. Xi, L.M. Graça, Infrared and Raman spectroscopic characterization of the borate mineral hydroboracite CaMg $[B_3O_4 (OH)_3]_2 \cdot 3H_2O$—implications for the molecular structure. J. Mol. Struct. **1059**, 20–26 (2014)

27. R.C. Lucacel, I. Ardelean, Comparative structural investigation of B_2O_3–MO–CuO glasses (MO → TeO_2 or As_2O–3) by FTIR and Raman spectroscopies. J. Optoelectron. Adv. Mater. **8**(3), 1124 (2006)

28. A. Samir, M.A. Hassan, A. Abokhadra, L. Soliman, M. Elokr, Characterization of borate glasses doped with copper oxide for optical application. Opt. Quant. Electron. **51**(4), 1–13 (2019)

29. C. Gautam, A.K. Yadav, A.K. Singh, A review on infrared spectroscopy of borate glasses with effects of different additives. Int. Schol. Res. Notices **2012**, 428497 (2012)

30. M.R. Joya, J. Barba, A. Raba, Vibrational Raman modes and particle size analysis of cupric oxide with calcination temperature. Indian J. Pure Appl. Phys. (IJPAP) **57**(4), 268–271 (2019)

31. V. Chekhovskii, Interpretation of the IR spectra of alkali borate glasses. Sov. J. Glass Phys. Chem. **11**, 1 (1985)

32. H. ElBatal, A. Abdelghany, I. Ali, Optical and FTIR studies of CuO-doped lead borate glasses and effect of gamma irradiation. J. Non-Cryst. Solids **358**(4), 820–825 (2012)

33. F. ElBatal, S. Marzouk, N. Nada, S. Desouky, Gamma-ray interaction with copper-doped bismuth–borate glasses. Physica B **391**(1), 88–97 (2007)

34. Y.B. Saddeek, E.R. Shaaban, H.M. Moustafa, Spectroscopic properties, electronic polarizability, and optical basicity of Bi2O3–Li2O–B2O3 glasses. Physica B **403**(13–16), 2399–2407 (2008)

35. U. Chanshetti, V. Sudarsan, M. Jogad, T. Chondhekar, Effect of CuO addition on the optical and electrical properties of sodium zinc borophosphate glasses. Physica B **406**(14), 2904–2907 (2011)

36. W. Abd-Allah, H. Saudi, K.S. Shaaban, H. Farroh, Investigation of structural and radiation shielding properties of $40B_2O_3$–30PbO–(30–x) BaO-x ZnO glass system. Appl. Phys. A (2019). https://doi.org/10.1007/s00339-019-2574-0

37. I. Kashif, A. Soliman, H. Farouk, M. El-Shorpagy, A. Sanad, Effect of copper addition on density and magnetic susceptibility of lithium borate glasses. Physica B **403**(21–22), 3903–3906 (2008)

38. H. ElBatal, A. Abdelghany, F. ElBatal, K.M. ElBadry, F. Moustaffa, UV–visible and infrared absorption spectra of gamma irradiated CuO-doped lithium phosphate, lead phosphate and zinc phosphate glasses: a comparative study. Physica B **406**(19), 3694–3703 (2011)

39. N. Mott, E. Davis, *Electronic processes in non-crystalline materials*, 2nd edn. (Clarendon, Oxford, 1979)

40 K. Aly, N. Afify, A. Abousehlly, A. AbdElnaeim, Optical band gap and refractive index dispersion parameters of In–Se–Te amorphous films. J. Non-Cryst. Solids **357**(10), 2029–2034 (2011)

41. M. Azlan, M. Halimah, S. Shafinas, W. Daud, Polarizability and optical basicity of Er^{3+} ions doped tellurite based glasses. Chalcogenide Lett **11**(7), 319 (2014)

42. M. Thombare, R. Joat, D. THombre, V. Mahavidyalaya, Glasses study physical properties of sodiumborophosphate. Int. J. Eng. Sci. 8482 (2016).

43. G. Baym, G. Brown, The Lorentz-Lorenz correction. Nucl. Phys. A **247**(3), 395–410 (1975)

44. S.W. McKeever, *Thermoluminescence of Solids* (Cambridge University Press, Cambridge, 1988)

45. J. Peng, Z. Dong, F. Han, tgcd: An R package for analyzing thermoluminescence glow curves. SoftwareX **5**, 112–120 (2016)

46. Z.G.P. Uçar, Thermoluminescence characteristics and kinetic analysis of beta irradiated Ca_4LaO $(BO_3)_3$ phosphor. Cumhuriyet Science Journal **42**(3), 702–714 (2021)

47. A. El-Bayoumi, H.A. Alazab, F. Ezz-ElDin, The impact of γ-irradiation on $Cd-B_2O_3$ glass doped WO_3: New evidences by TL and ESR spectroscopy. J. Non-Cryst. Solids **551**, 120459 (2021)

48 C. Furetta, *Handbook of Thermoluminescence* (World Scientific, Singapore, 2003)

49. S. Farouk, A. Gad, H. Al-Azab, H. El-Nashar, N. El-Faramawy, Thermoluminescence response and its kinetic analysis of a natural milky quartz associated with tin-tungsten-fluorite mineralization. Radiat. Phys. Chem. **181**, 109333 (2021)

50. S.W. McKeever, M. Moscovitch, P.D. Townsend, Thermoluminescence dosimetry materials: properties and uses. J. Radiol. Protect. (1995). https://doi.org/10.1088/0952-4746/16/4/018